Draft version October 29, 2013
Preprint typeset using LaTeX style emulateapj v. 5/25/10

MAGNETIC RECONNECTION RATE IN TWO AND THREE DIMENSIONAL RESISTIVE MHD SIMULATIONS

M. Čemeljić, R.-Y. Huang
Academia Sinica, Institute of Astronomy and Astrophysics and Theoretical Institute for Advanced Research in Astrophysics, P.O. Box 23-141, Taipei 106, Taiwan
Draft version October 29, 2013

ABSTRACT

By a direct comparison between numerical simulations in two and three dimensions, we investigate topological effects in the rate of reconnection.

Subject headings: methods: numerical — processes: MHD

1. INTRODUCTION

Reconnection of magnetic field is a process in which magnetic field lines change connection with respect to the sources. In effect, magnetic energy is converted into kinetic and thermal energies, which accelerate and heat the plasma. Reconnection is assumed and observed in

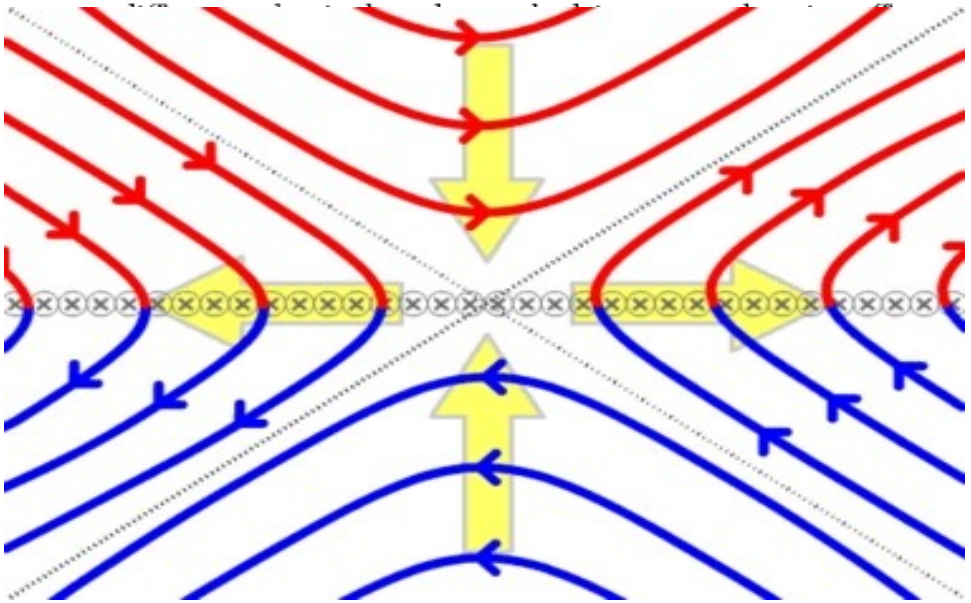

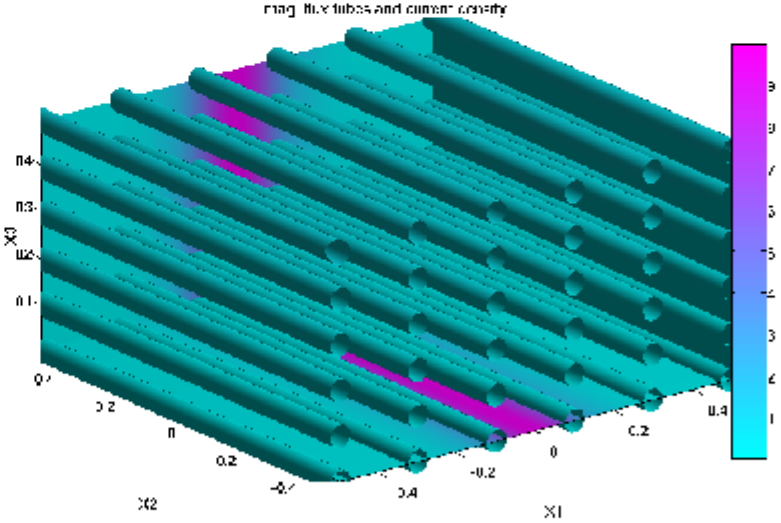

Fig. 1.— Setup of initial and boundary conditions in our simulations in three dimensions. In two dimensional simulations, X3=0. In color grading is shown a current density at the boundary planes; tubes show the magnetic flux tubes, with the diameter of the tube set proportional to the magnetic field strength.We start with a 3D simulation in Cartesian coordinates $X_1 \times X_2 \times X_3$. Then we decrease the height of a box in X3 direction, and compare the reconnection rates, until we reach a 2D simulation in $X_1 \times X_2$.

However, his model fails in explanation of solar flares

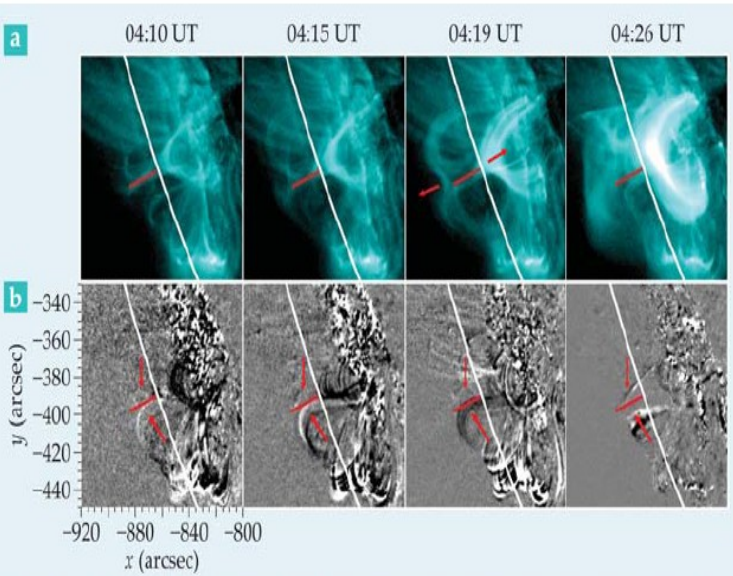

Figure 2. Images of a flare captured by the Atmospheric Imaging Assembly (AIA) on the *Solar Dynamics Observatory*. The flare erupted on 17 August 2011 near the visible edge of the solar disk, shown by the white curve. **(a)** The AIA's 131-Å channel imaged the loops of hot plasma flowing outward from the reconnection region (red line). **(b)** Difference images derived from the lower-energy extreme UV channels show loops of relatively cool plasma flowing inward toward the reconnection region. (Adapted from ref. 1.)

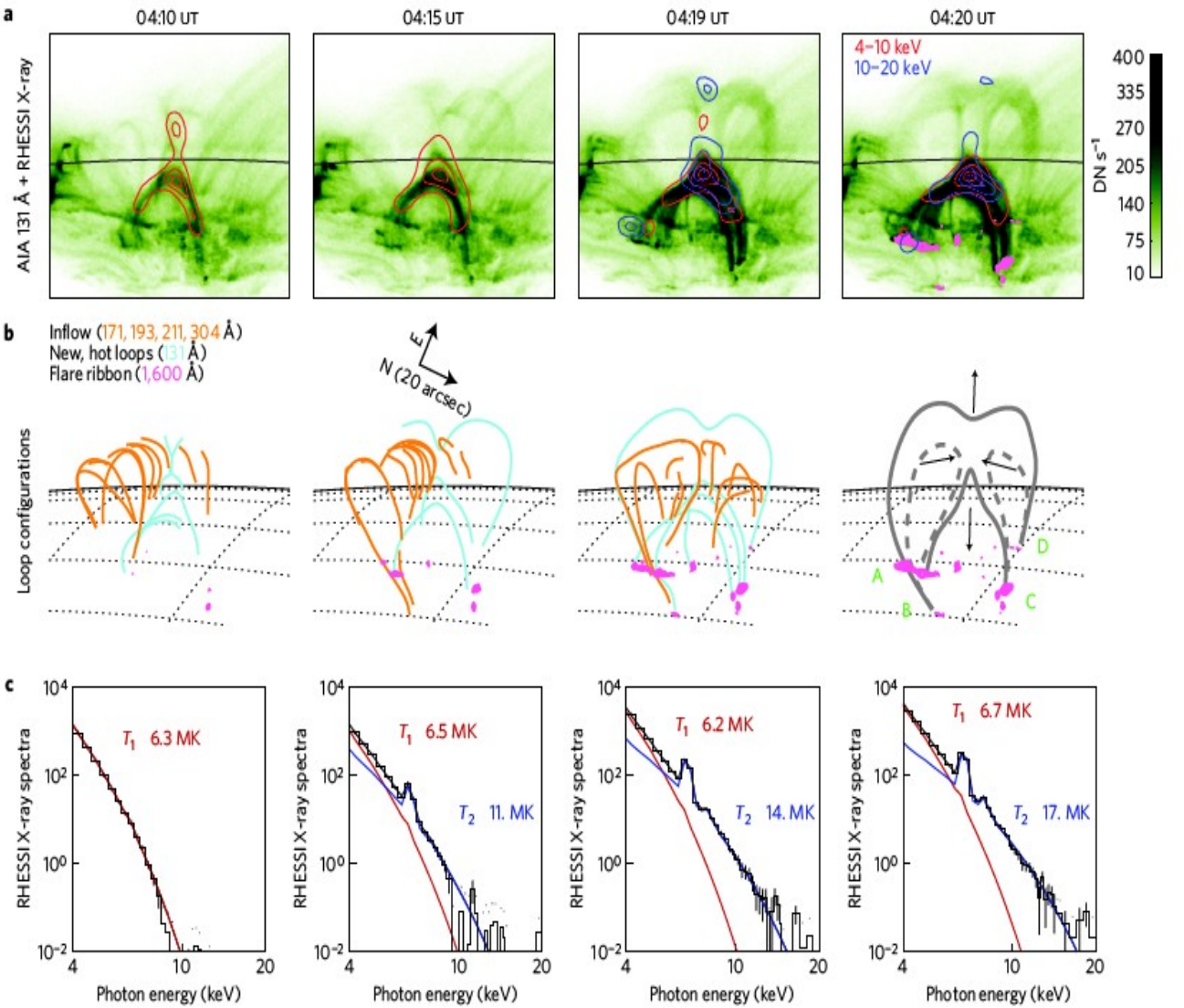

Figure 2 | The reconnection and energy release imaged by SDO/AIA in EUV and RHESSI in X-rays. The combination of data from different wavelengths shows the entire sequence of events expected for reconnection. **a**, AIA 131 Å images, taken from Supplementary Movie 4, show the formation of the new hot loops. The images are rotated clockwise by 114° to orient the solar limb (black line) in the horizontal direction. RHESSI X-ray fluxes[29] are shown as red (blue) contours in the 4–10 (10–20) keV bands at 10, 40 and 80% of the maximum in each image. Bright flare regions on the surface observed at AIA 1,600 Å are superposed in pink in the fourth image. **b**, The evolution of loop configurations. Orange lines show the major inflow loops derived from AIA images at 171, 193, 211 and 304 Å; cyan lines show the hot loops and cusps in the AIA 131 Å images. Main flare regions (pink) are marked by A, B, C and D (see Supplementary Fig. S1). The dashed grey lines in the fourth image illustrate the inflowing cool loops; the solid grey lines illustrate the newly formed loops after the reconnection. Arrows indicate flow directions. **c**, RHESSI X-ray spectra of the heated plasma. The measured background-subtracted spectra (photons s^{-1} cm^{-2} keV^{-1}) are shown as histograms with error bars. The temperatures (T_1 and T_2) of two isothermal components (red and blue lines) that, summed together (black lines), give the best fit to the data are shown for each spectrum.

$$\frac{\partial \rho}{\partial t} + \nabla \cdot (\rho \boldsymbol{V}) = 0 \quad (1)$$

$$\rho \left[\frac{\partial \boldsymbol{V}}{\partial t} + (\boldsymbol{V} \cdot \nabla) \boldsymbol{V} \right] + \nabla p - \frac{\boldsymbol{j} \times \boldsymbol{B}}{c} = 0 \quad (2)$$

$$\frac{\partial \boldsymbol{B}}{\partial t} - \nabla \times \left(\boldsymbol{V} \times \boldsymbol{B} - \frac{4\pi}{c} \eta \boldsymbol{j} \right) = 0 \, , \nabla \cdot \boldsymbol{B} = 0 \quad (3)$$

$$\rho \left[\frac{\partial e}{\partial t} + (\boldsymbol{V} \cdot \nabla) e \right] + p(\nabla \cdot \boldsymbol{V}) - \frac{4\pi}{c^2} \eta \boldsymbol{j}^2 = 0 \, , \quad (4)$$

PLUTO, resistive MHD equations in Cartesian coordinates, with ideal eq. of state. “Dimensional splitting” option, which uses Strang operator splitting to solve the multi-dimensional eqs. “LINEAR” spatial order od integration is used, so that a piecevise TVD linear interpolation is applied, accurate to second order in space. RK2 evolution scheme with the Eight-Waves option for constraining div B=0 is used, with Lax-Friedrich approximate Riemann solver.

$$\eta = (\eta_0 - \eta_1) \exp\left[-(x_1/a_1)^2 - (x_2/a_2)^2 \right] \quad (5)$$

$$+(\eta_0 - \eta_1) \exp -(x_1/a_1)^2 - (x_3/a_3)^2 + \eta_1$$

$$= \eta_1 + (\eta_0 - \eta_1) \exp\left[-(x_1/a_1)^2 \right]$$

$$\cdot \left(\exp\left[-(x_2/a_2)^2 \right] + \exp\left[-(x_3/a_2)^2 \right] \right) \, ,$$

Resistivity is set as asymmetric in both horizontal and vertical planes.

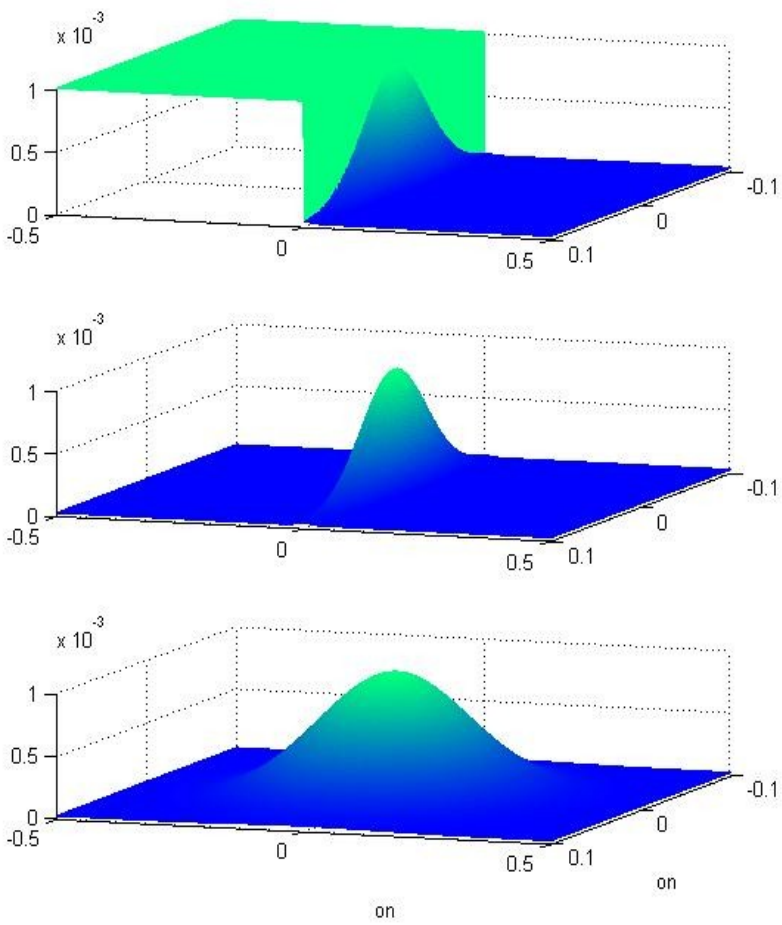

Three different cases of resistivity setups in 2D: the case of asymmetric, small and large resistivity, respectively, top to bottom panels.

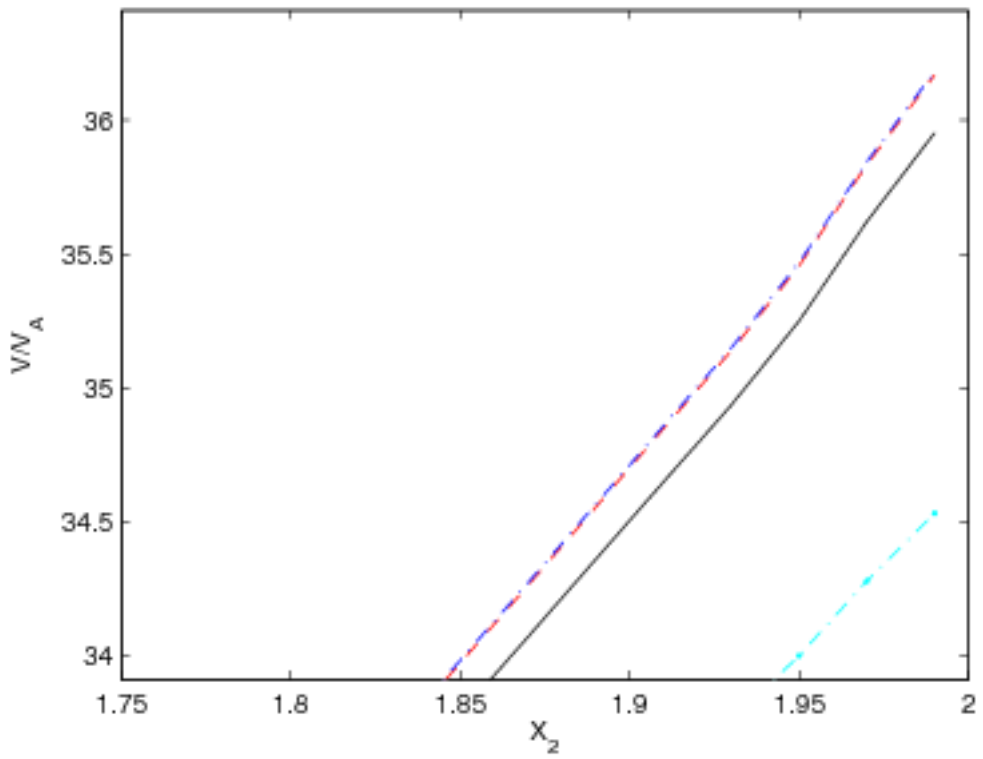

at T=20 and T=50, respectively. The ratios are computed along the X_2 direction at $X_1 = 0$. In the *right* panel is shown a zoom into the difference in the results for this ratio, at the exiting portion of the computational box at T=50, for the various values of resistivity in (cyan) dot-dashed, (black) solid, (red) dashed and (blue) dot-dashed for $\eta = (10, 1, 0.1, 0.01) \cdot 10^{-5}$. This is the illustration for the threshold of numerical resistivity, and overlap of the result for $\eta = 0.1 \cdot 10^{-5}$ and $0.01 \cdot 10^{-5}$ shows that numerical resistivity in our simulations is of the order of $\eta_{num} = 0.1 \cdot 10^{-5}$. We performed all our simulations with the minimum value of the resistivity set for an order of magnitude above the numerical resistivity.

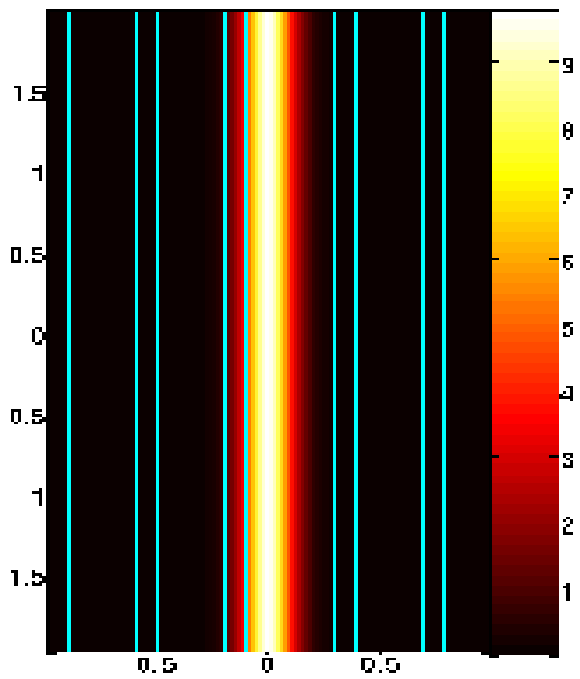

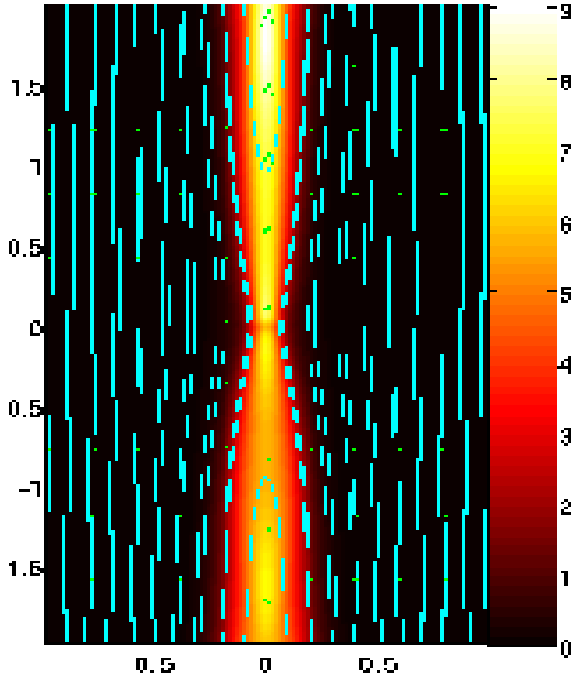

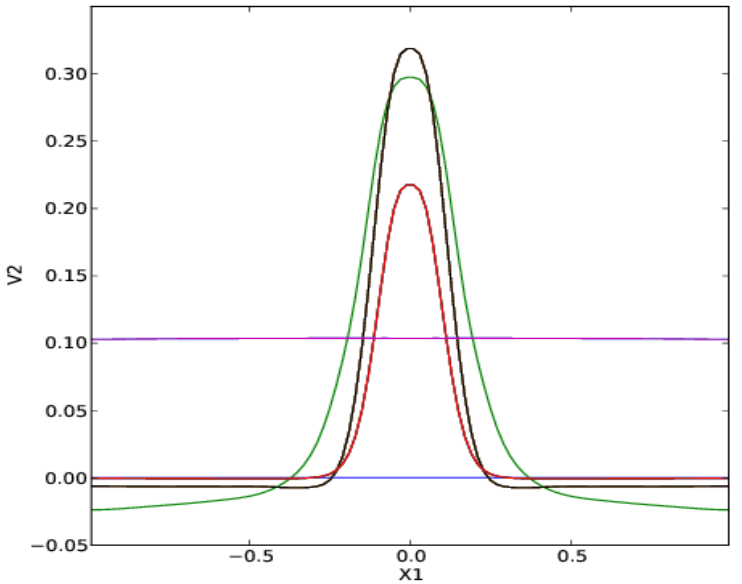

Reconnection in two dimensions, with current density shown in color grading, magnetic field contour lines in solid lines and arrows showing velocity. In the left panel is initial setup, and right is the result at T=100.

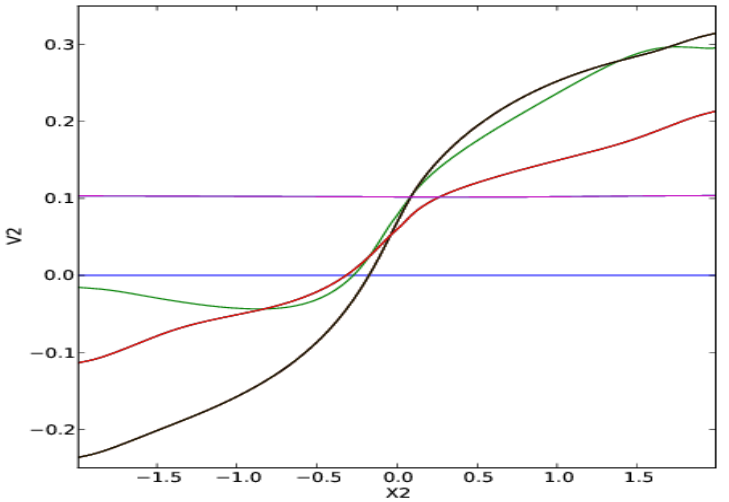

V2 along the direction X1 at x2= 2.0 (Top), and along the direction X2 at x1 = 0 (Bottom). In blue, green, red, black and violet solid lines are V2 at times T=0,20,50,100 and 500. At T=500 magnetic field is reorganized, flow is perpendicular to the initial direction.

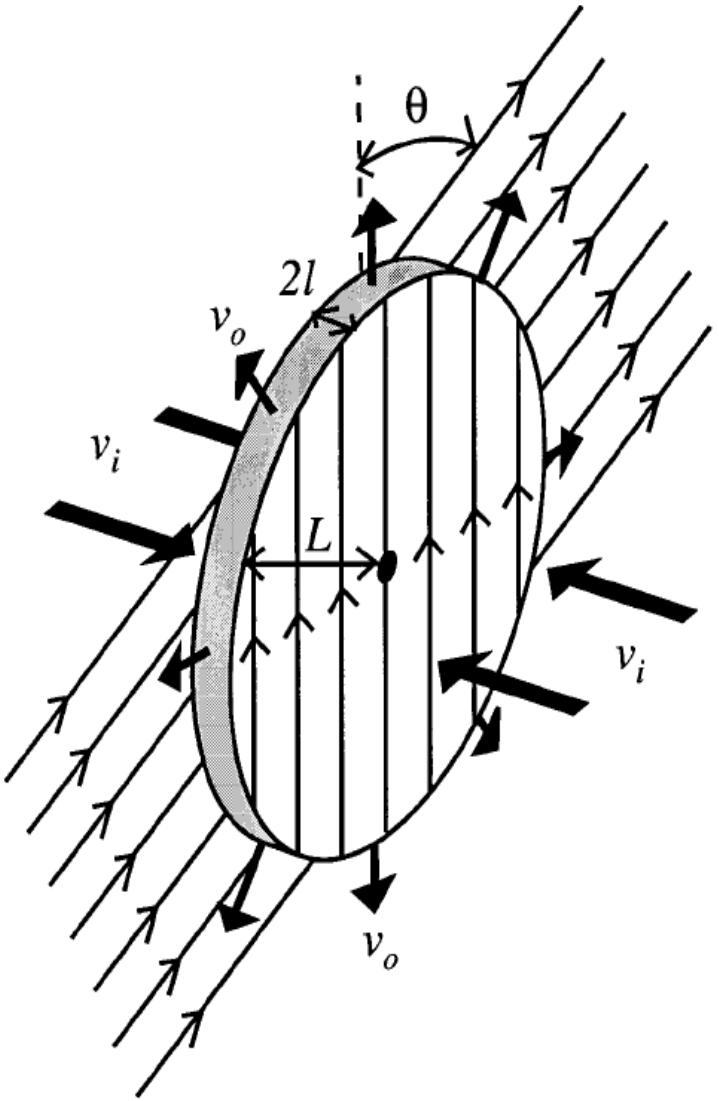

Figure 8. The three-dimensional reconnection of two flux tubes inclined at an angle θ. The field lines of one tube are shown on the front side of a disc-shaped diffusion region and of the other tube behind the disc.

In a simple 3D case, similar reconnection rate as in 2D can be derived, with the maximum value √2 times larger than in 2D.

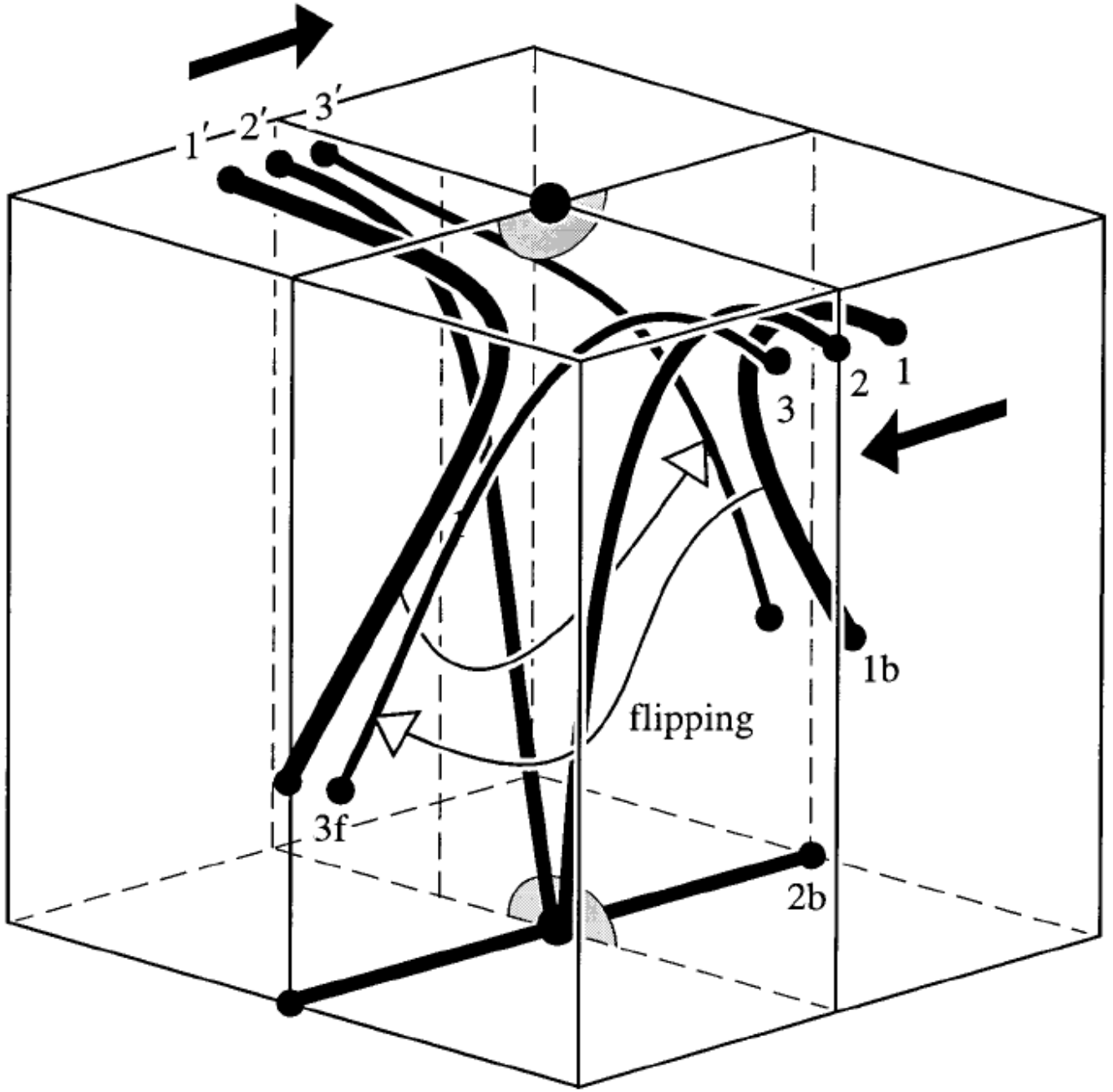

Figure 7. Rapid counter-flipping of field lines caused by small footpoint motions on the left- and right-hand sides of a box. One null point and its spine lies on the top side and another lies on the bottom of the box. Footpoints move from 1 to 2 to 3 on the right-hand side and from 1′ to 2′ to 3′ on the left-hand side. This forces the field lines through those footpoints to flip from the back of the box (1b and 2b) to the front (3f), and vice-versa, and to reconnect at the lower null point.

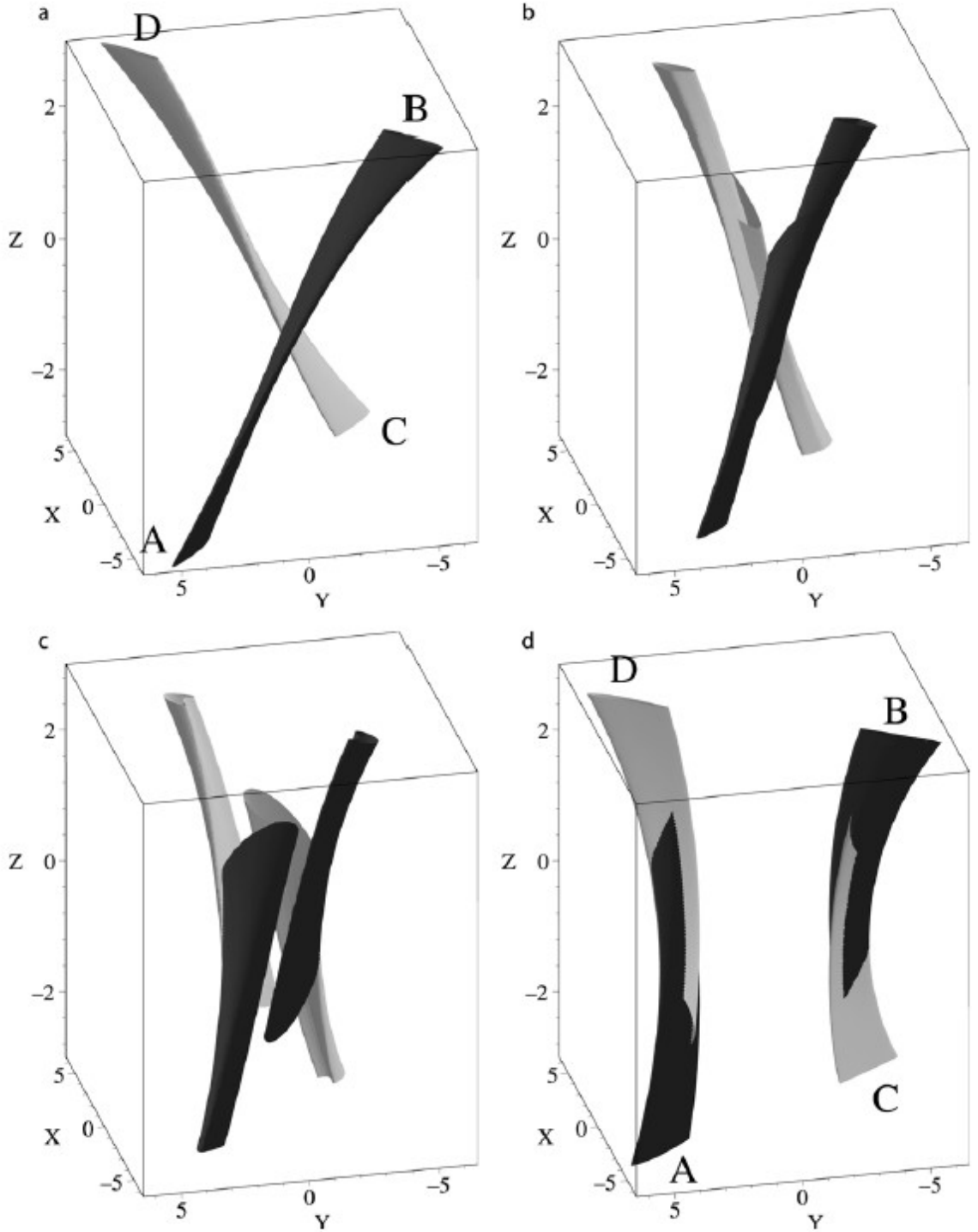

Figure 8. Kinematic reconnection of two flux tubes (integrated from the cross sections A, B, C and D) for the magnetic field $\mathbf{B} = (y, k^2x, b_0)$. (a) The initial two tubes. (b) The tubes start to split and (c) the tubes flip past each other. (d) The final four nonmatching flux tubes once they have left the diffusion region.

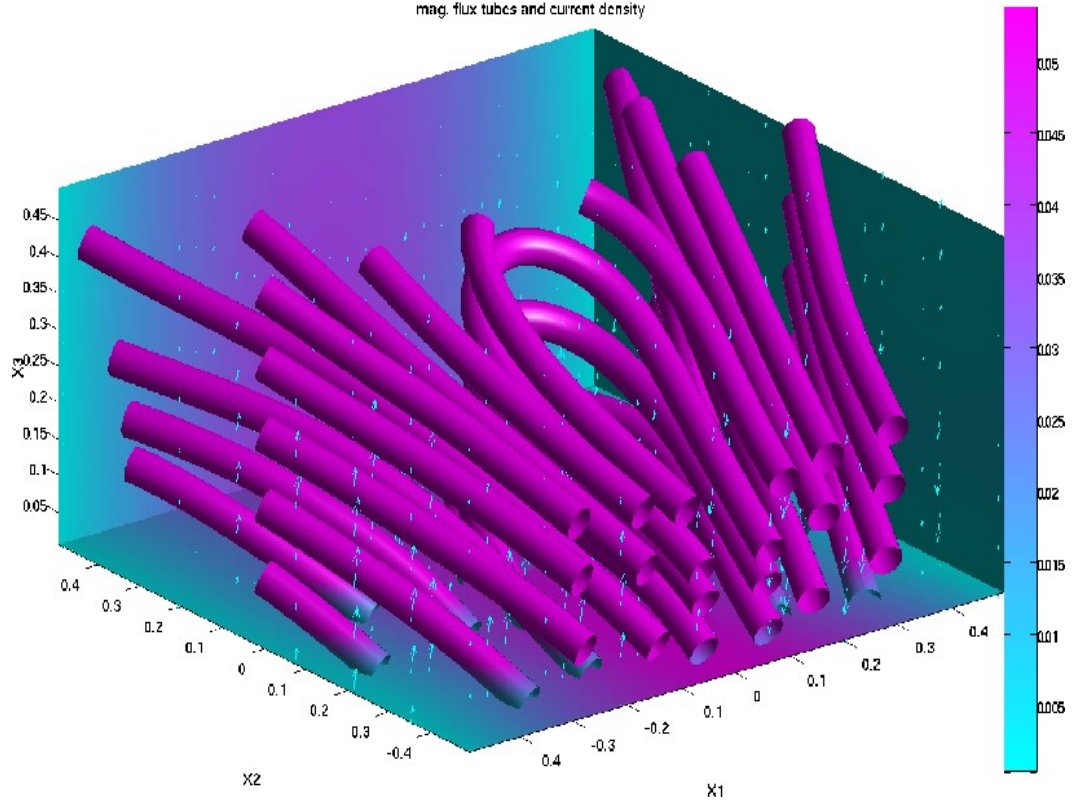

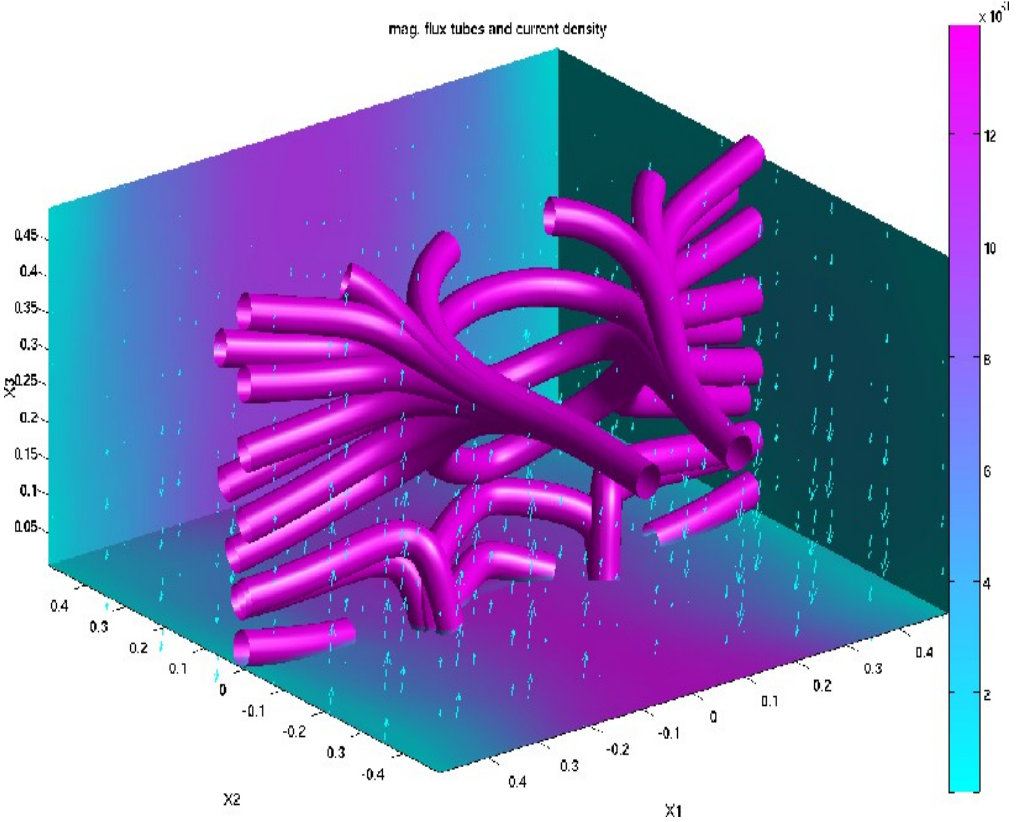

My solutions in 3D at T=40 and T=52. In color grading is shown the toroidal current density at the boundary planes; tubes show the magnetic flux tubes, with the diameter of the tube set proportional to the magnetic field strength. A change in connectivity of the magnetic flux tubes in the third dimension is a change in topology of magnetic field.

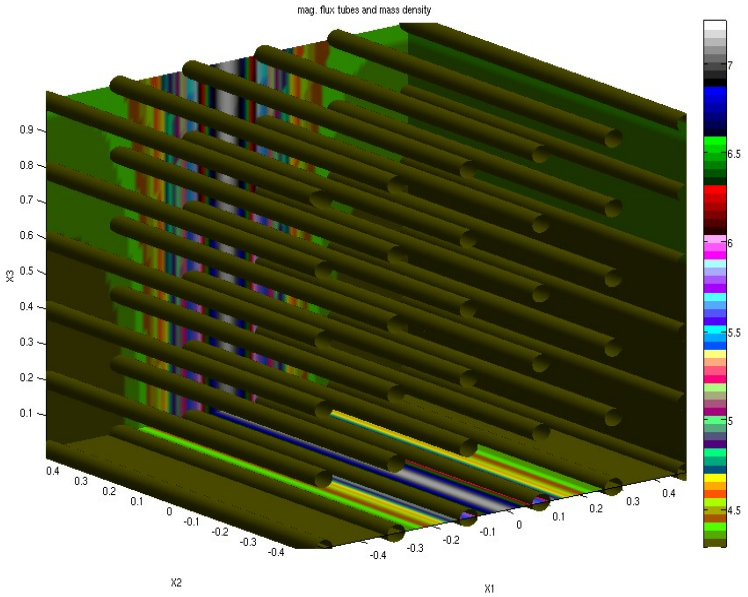

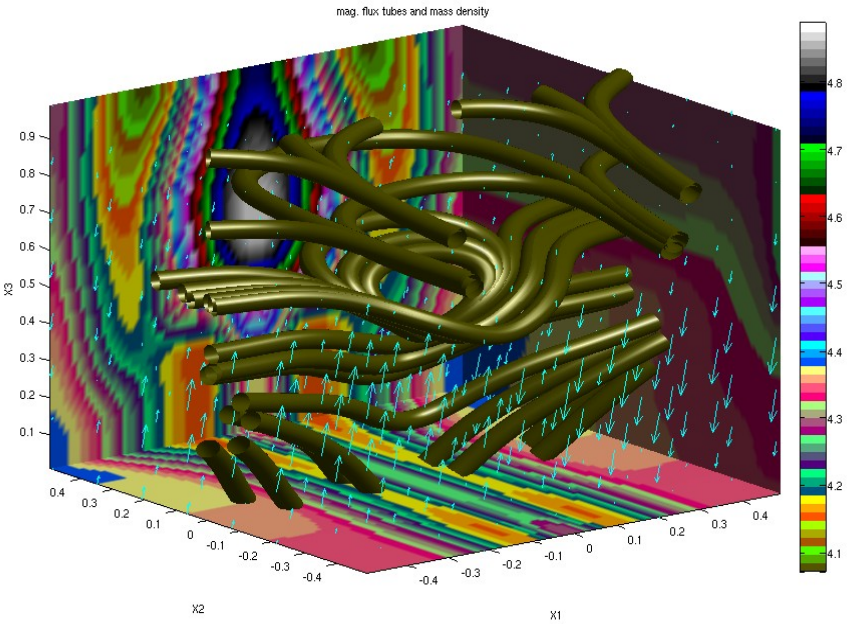

Still missing: conclusive results about the rate of reconnection. I am still searching for the best measure for it, which would not be so much model dependent. Probably it will be some energy density consideration, but I did not know how to test if it works. Now I know that it should be something like √2 times the value from 2D simulation. Still to be verified.